Tunneling recombination and the photoconductivity of amorphous silicon in the temperature region around 100 K

J.-H. Zhou*
Department of Chemistry, University of Cambridge, Lensfield Road, Cambridge CB2 1EW, United Kingdom and Department of Electrical and Computer Engineering, Faculty of Technology, Kanazawa University, 2-40-20 Kodatsuno, Kanazawa 920, Japan

S. R. Elliott
Department of Chemistry, University of Cambridge, Lensfield Road, Cambridge CB 1EW, United Kingdom
(Received 27 August 1992; revised manuscript received 9 February 1993)

This paper proposes an interpretation of the photoconductivity of *a*-Si:H *in the temperature region between* ~50 *and* ~150 *K*, where the photoconductivity increases rapidly with temperature and usually exhibits a thermally activated behavior. In this model, the recombination takes place by direct tunneling between electrons and holes trapped in the band tails, whereas the photoconductivity is due to electron conduction in extended states. It is shown that this model can account for all the general features exhibited by the photoconductivity of *a*-Si:H in the low-temperature region, although the magnitude of the photoconductivity predicted by the model tends to be larger than that measured.

I. INTRODUCTION

Photoconductivity has been a major subject in the research into hydrogenated amorphous silicon (*a*-Si:H) over the last 15 years or so. However, the interpretation of the photoconductivity data is still a matter of considerable debate. Figure 1 illustrates schematically the typical temperature dependence of the photoconductivity of *a*-Si:H. Usually, four distinct regimes appear in the temperature dependence of the photoconductivity,[1-5] as labeled in the figure. At very low temperatures (regime I), the photoconductivity is almost independent of temperature. In the regime II, the photoconductivity increases rapidly with increasing temperature. This is followed by the regime III where either a shoulder[1,2] or a decreasing photoconductivity,[3-5] known as thermal quenching,[6] occurs. At still higher temperatures, the photoconductivity changes and rapidly increases with temperature again. The values of the transition temperatures between the regimes, T_1, T_2, and T_3 (marked in Fig. 1), depend on the sample. For high-quality *a*-Si:H, T_1 is about 60 K.[1,4,5] However, T_2 and T_3 are also dependent upon the excitation intensity and increase with increasing excitation intensity.[1] For example, at a generation rate of 10^{20} $cm^{-3}s^{-1}$, T_2 is about 250 K.[1]

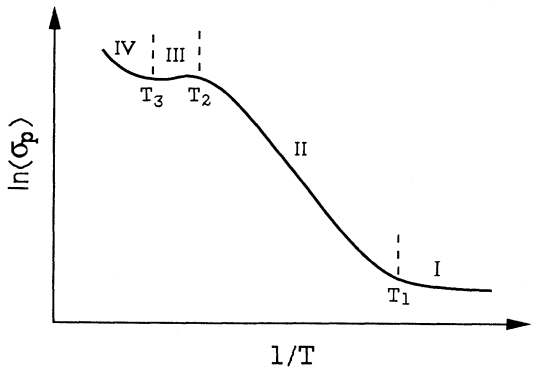

FIG. 1. Schematic illustration showing the temperature dependence of the photoconductivity of *a*-Si:H. The different regimes are labeled by I, II, III, and IV. T_1, T_2, and T_3 denote the transition temperatures between the different regimes.

The photoconductivity in the high-temperature regimes III and IV has been studied the most. There is a large volume of literature on the photoconductivity typically around room temperature. In the very-low-temperature regime I, the photoconductivity is believed to be due to electron hopping conduction in the conduction-band-tail states and has been discussed in some depth in a number of recent studies.[7-10] In this paper, we are concerned with the photoconductivity in the regime II.

As can be seen from Fig. 1, the regime II covers a large temperature range, typically between 250 and 50 K. It has been established that the photoconductivity in the regime II possesses the following features.

(a) The photoconductivity increases rapidly with temperature. Usually, the temperature dependence of the photoconductivity can be described by a thermally activated behavior, with the activation energy being about 0.11 eV.[1,3,4]

(b) The activation energy appears to be independent of the excitation intensity.[1,3]

(c) The recombination is bimolecular in nature, i.e., the exponent γ, defined by $\gamma = d\ln(\sigma_p)/d\ln(G)$, is close to 0.5,[4,5,9] where σ_p is the photoconductivity and G is the carrier generation rate.

(d) Unlike the photoconductivity at high temperatures (regimes III and IV), the photoconductivity in the regime II is little affected by intense light soaking,[1,4] which is known to create recombination centers lying deep in the

band gap.[11]

Usually, the temperature dependence of the photoconductivity in the regime II is explained in terms of the band-tail-recombination model.[1,12–14] In this model, it is argued that, as the quasi-Fermi-levels move towards their respective mobility edges with decreasing temperature, increasing numbers of band-tail states are brought into play as recombination centers, which decrease the photoconductivity. Obviously, since the band-tail-recombination model does not involve the deep recombination centers, feature (d) above can be accounted for easily by this model. We have shown that, indeed, a good agreement between the band-tail-recombination model and the photoconductivity can be obtained for the high temperatures in the regime II, typically between 250 and 150 K.[1] However, the band-tail-recombination model has some serious difficulties. First, for the low temperatures in the regime II, the predicted temperature dependence of the photoconductivity is far too weak compared with that observed and cannot be approximated by an activated form.[1,12–14] Second, the exponent γ is predicted to increase monotonically with decreasing temperature[15] and to become close to unity below 100 K if an exponential form is taken for the energy distribution of the conduction-band-tail states,[16] regardless of the generation rate. In principle, the first difficulty can be overcome by introducing an energy dependence for the capture cross section of the tail states.[13,14] However, despite the fact that there has been some evidence for an energy-dependent capture cross section of the tail states, little is known about the form of such an energy dependence. Various energy dependences have been used by different authors to meet their particular needs.[12–14]

In contrast, Vomvas and Fritzsche[4] argue that the recombination in the regime II is not by capture of free electrons from extended states, but by tunneling of trapped electrons at a dominant trap level in the conduction-band tail[17] to the deep recombination centers—the dangling bonds.[18] Although the thermally activated behavior of the photoconductivity [feature (a)] and the excitation-intensity-independent activation energy [feature (b)] seem in favor of the tail-to-dangling-bond-recombination model, obviously the insensitivity of the photoconductivity to intense light soaking [feature (d)] stands against it. In addition, it is not clear how the photoconductivity varies with the excitation intensity in the tail-to-dangling-bond-recombination model.

In this paper, we consider a recombination model in which the recombination is dominated by direct tunneling between trapped electrons and trapped holes in the band-tail states. Assuming the existence of quasithermal equilibrium between free and trapped electrons, we show that all the features exhibited by the photoconductivity in the regime II can be accounted for by this tail-to-tail-tunneling-recombination (TTTR) model.

II. MODEL

A. Formulation

The mechanism of direct tunneling recombination between band-tail electrons and holes is not new; this process is known to be responsible for the luminescence in *a*-Si:H.[19] It has been observed[20] that the low-temperature luminescence in *a*-Si:H is independent of the defect density when the defect density is smaller than 10^{17} cm^{-3}. Since in high-quality *a*-Si:H the defect density is normally below 10^{16} cm^{-3}, we assume that the dominant recombination channel is tail-to-tail tunneling.

Obviously, since the TTTR model does not involve the deep defect states, the insensitivity of the photoconductivity of *a*-Si:H to intense light soaking [feature (d)] can be readily understood with this model, as with the band-tail-recombination model.[1]

The tunneling rate is given by[19]

$$\nu_T=\nu_0\exp(-2R/R_0)\ , \tag{1}$$

where R is the separation between the trapped electron and hole, R_0 is the localization length or effective Bohr radius, and ν_0 is a prefactor. Usually, the hole is assumed to be more localized than the electron in *a*-Si:H; thus R_0 in Eq. (1) can be regarded as the localization length of the electron. For radiative recombination, ν_0 is of order 10^8 s^{-1}, and for nonradiative recombination ν_0 is often assumed to be about 10^{12} s^{-1} (Ref. 19). It should be noted that, in general, both radiative and nonradiative recombination can occur. Thus, ν_0 in Eq. (1) should be treated as an effective tunneling-rate prefactor and can take any value between 10^8 and 10^{12} s^{-1} to take account of the combined effect of radiative and nonradiative recombination. The value of ν_0 will be estimated later in Sec. III based on the photoluminescence data in the literature.

Since the tunneling rate decreases exponentially with the separation between the electron and hole, we can assume that recombination only occurs between the nearest neighbors. Let n_t and p_t be, respectively, the densities of trapped electrons in the conduction-band-tail states and of trapped holes in the valence-band-tail states. At low temperatures, the free-carrier densities are small compared with the trapped-carrier densities, and charge neutrality requires that $n_t=p_t$. The average nearest-neighbor separation between electrons and holes in the case of equal numbers of electrons and holes can be estimated by using different methods and has the general form

$$R=B/n_t^{1/3}\ . \tag{2}$$

Often, a nonrigorous method is used, in which electrons and holes are assumed to be uniformly distributed in the material. By approximating the average space occupied by a carrier to a sphere, one obtains $B=(3/4\pi)^{1/3}\approx 0.62$. Approximation of the average space occupied by a carrier to a cube gives rise to $B=\sqrt{3}/2\approx 0.87$. Here, we adopt a more rigorous approach. The distribution function of the nearest-neighbor separations for a randomly distributed collection of equal numbers of electrons and holes is given by[19,21]

$$g(R)=4\pi R^2 n_t\exp(-4\pi R^3 n_t/3)\ . \tag{3}$$

From Eq. (3), the most probable nearest-neighbor separation is

$$R_m=1/(2\pi n_t)^{1/3}\ . \tag{4}$$

Thus, for the method used here, $B=1/(2\pi)^{1/3}\approx 0.54$.

Insertion of Eq. (2) into Eq. (1) yields

$$\nu_T=\nu_0\exp(-2B/R_0 n_t^{1/3}) . \tag{5}$$

If G is the carrier-generation rate, then

$$n_t=G/\nu_T=(G/\nu_0)\exp(2B/R_0 n_t^{1/3}) . \tag{6}$$

Assume that the tunneling recombination takes place predominantly nongerminately and that there exists quasithermal equilibrium between free and trapped electrons. In the steady state under illumination, there must exist a filling level E_{fn} so that the occupancy of the tail states below E_{fn} is essentially unity and the occupancy of the states above E_{fn} can be approximated by the Boltzmann function. As can be seen below, E_{fn} provides a link between the free-electron density n and the trapped-electron density n_t. Assume, as one usually does, that the energy distribution of the conduction-band-tail states is exponential,[16] i.e.,

$$N_t(E)=N_0\exp[-(E_c-E)/kT_c] , \tag{7}$$

where N_0 is the extrapolated trap density of states at the conduction-band mobility edge E_c, k is the Boltzmann constant, and T_c is the characteristic temperature of the conduction-band tail. A straightforward calculation of the density of occupied conduction-band-tail states leads to

$$n_t\approx\frac{kT_cN_0}{1-\alpha_c}\exp[-(E_c-E_{fn})/kT_c] , \tag{8}$$

where $\alpha_c=T/T_c$.

The density of free electrons can be expressed in terms of E_{fn},

$$n=kTN_0\exp[-(E_c-E_{fn})/kT] , \tag{9}$$

where N_C is the density of states at E_c. In writing Eq. (9), we have taken into account the possibility that the distribution of the density of states close to the mobility edge may deviate from the exponential form and that, therefore, the density of states at the mobility edge, N_c, may be different from the extrapolated trap density of states at the mobility edge, N_0. From Eqs. (8) and (9) we have

$$n_t=\frac{kT_cN_0}{(1-\alpha_c)(kTN_c)^{\alpha_c}}n^{\alpha_c} . \tag{10}$$

Substitution of Eq. (10) into Eq. (6) yields

$$\frac{kT_cN_0n^{\alpha_c}}{(1-\alpha_c)(kTN_c)^{\alpha_c}}=G\tau_0\exp\left\{\frac{2B}{R_0}\left[\frac{(1-\alpha_c)(kTN_c)^{\alpha_c}}{kT_cN_0n^{\alpha_c}}\right]^{1/3}\right\} . \tag{11}$$

The dependence of n on the various parameters, such as temperature and excitation intensity, are implicitly contained in Eq. (11) and can be resolved numerically. It is worth pointing out, however, that Eq. (11) is not a good point with which to start the numerical calculation because it is somewhat too complicated. Instead, one starts with Eq. (6) to find out first the n_t for a given generation rate G. Then, Eq. (10) is used to obtain the temperature dependence of n. If we neglect the contribution of hopping conduction,[9] the photoconductivity is then proportional to the free-electron density n according to

$$\sigma_p=ne\mu_e , \tag{12}$$

where e is the electronic charge and μ_e is the extended-state mobility of electrons.

B. Further analysis

In principle, Eq. (11), or equivalently Eqs. (6) and (10), can serve as a master equation to obtain the dependence of the free-carrier density and thus of the photoconductivity on any of the parameters involved through numerical calculation. However, insights into these dependences can be gained by a more detailed analysis of the TTTR model.

Equation (6) indicates that, for a given generation rate G, n_t is constant irrespective of the temperature. This is a consequence of the assumption that the tunneling rate is temperature independent [Eq. (1)]. Rewriting Eq. (10) we have

$$\begin{aligned} n&=kTN_c\exp\left\{-\frac{1}{\alpha_c}\ln\left[\frac{kT_cN_0}{(1-\alpha_c)n_t}\right]\right\} \\ &=kTN_c\exp\left\{-kT_c\ln\left[\frac{kT_cN_0}{(1-T/T_c)n_t}\right]\Big/kT\right\} , \end{aligned} \tag{13}$$

replacing α_c with T/T_c. Seemingly, the photoconductivity is not expected to exhibit a simple thermally activated behavior except at very low temperatures, say $T<T_c/5$, where $(1-T/T_c)\approx 1$. The very-low-temperature photoconductivity activation energy is, according to Eq. (13), given by

$$E_a(T\rightarrow 0)=kT_c\ln(kT_cN_0/n_t) . \tag{14}$$

The photoconductivity activation energy at any temperature T is defined as

$$E_a(T)=-d\ln(n)/d(1/kT) . \tag{15}$$

Using Eq. (13) we obtain

$$E_a(T)=E_a(T\rightarrow 0)-kT_c\ln(1-T/T_c)-kT^2/(T_c-T) . \tag{16}$$

It can be easily shown that $E_a(T)$ is essentially constant and is slightly larger than $E_a(T\rightarrow 0)$ unless $T>2T_c/3$. Thus, for $T_c=300$ K,[16] the photoconductivity is expected to show a well-defined activation energy below 200 K.

It is clear from Eq. (14) that a strong influence on E_a comes from T_c. Another parameter playing an equally important role in determining E_a is the localization length R_0, on which n_t depends exponentially. All the

other parameters have a much weaker effect on E_a because E_a is only logarithmically dependent on them.

The exponent γ in the intensity dependence of the photoconductivity is defined as

$$\gamma = d\ln(n)/d\ln(G) . \tag{17}$$

Using Eqs. (10) and (6) we have

$$\gamma = [d\ln(n)/d\ln(n_t)][d\ln(n_t)/d\ln(G)]$$
$$= T_c/[T(1+2B/3R_0 n_t^{1/3})] . \tag{18}$$

γ is a weak function of G because n_t is only weakly dependent on G. However, Eq. (18) shows that γ is strongly temperature dependent, increasing with decreasing temperature.

III. RESULTS

A. Determination of the values of the parameters

In order to calculate the photoconductivity and related quantities, we need to determine the values of the parameters involved. From Sec. II, $B=0.54$. For some of the parameters, the values can be found in the literature. We take $N_0=10^{21}$ cm^{-3}eV^{-1},[22] $T_c=300$ K,[16] and $\mu_e=10$ cm^{2}V^{-1}s^1.[16] The values of the rest of the parameters are determined below.

Many authors have suggested that the density of states immediately below the band edge is only weakly dependent on energy.[16,22,23] Although the exact width of this slowly-varying-density-of-states region is not clear, a width of 0.06 eV would imply that the density of states at the mobility edge, N_c, is some ten times smaller than the extrapolated trap density of states, N_0. For this reason, we take $N_c=10^{20}$ cm^{-3}eV^{-1}.

As mentioned in Sec. II both radiative and nonradiative recombination can take place through tunneling. If, at a given time, the proportion of the number of recombination channels that are radiative is χ, then the proportion of the recombination channels that are nonradiative is $1-\chi$. Since recombination is assumed to occur only between the nearest neighbors, the quantum efficiency of the photoluminescence can be expressed as

$$\eta_{PL}=\chi_{0R}/[X\nu_{0R}+(1-X)\nu_{0N}] , \tag{19}$$

where $\nu_{0R}=10^8$ s^{-1} and $\nu_{0N}=10^{12}$ s^{-1} are, respectively, the radiative- and nonradiative-tunneling-rate prefactors. The photoluminescence quantum efficiency at low temperatures has been measured by many researchers.[24–28] It seems reasonable to take $\eta_{PL}=20\%$. Then, we have from Eq. (19), $X=99.96\%$. This is to say that essentially all the tunneling recombination channels are radiative and only 0.04% are nonradiative, despite the fact that the nonradiative-recombination rate is much larger than the radiative-recombination rate. This is not surprising, because the tunneling-rate prefactor for nonradiative recombination is many orders of magnitude larger than that for radiative recombination and, therefore, even a relatively small number of nonradiative-recombination channels can lead to a large nonradiative-recombination rate and result in a large decrease in the photoluminescence quantum efficiency. It follows that the effective tunneling-rate prefactor is

$$\nu_0=\chi\nu_{0R}+(1-X)\nu_{0N}=5\times10^8 \text{ s}^{-1} . \tag{20}$$

The last parameter to determine is the localization length R_0. This was done by choosing the value of R_0 so that the calculated photoconductivity has the same activation energy as the observed. The value so determined is $R_0=8.5$ Å.

For clarity, we list the values chosen for the parameters in the calculation in the following: $N_0=10^{21}$ cm^{-3}eV^{-1}, $N_c=10^{20}$ cm^{-3}eV^{-1}, $T_c=300$ K, $B=0.54$, $\nu_0=5\times10^8$ s^{-1}, $R_0=8.5$ Å, and $\mu_e=10$ cm^{2}V^{-1}s^{-1}.

B. Results

Figure 2 shows the calculated temperature dependence of the photoconductivity in the temperature region between 60 and 160 K for three generation rates: 10^{18}, 10^{19}, and 10^{20} cm^{-3}s^{-1}. One can see clearly the thermally activated behavior of the photoconductivity. The photoconductivity activation energies for the three generation rates are, respectively, 0.121, 0.111, and 0.103 eV, in excellent agreement with the experimental observation that the activation energy is about 0.11 eV.[1,3,4] The activation energy E_a is seen to decrease with increasing generation rate, but the dependence is very weak.

It can also be shown that the photoconductivity is not a simple power-law function of G over a wide range of generation rates. However, a simple power-law behavior will be a good approximation for a small range of G, covering, for instance, three orders of magnitude or less. The temperature dependence of the exponent γ defined by Eq. (17) is shown in Fig. 3, for three carrier generation rates; 10^{17}, 10^{19}, and 10^{21} cm^{-3}s^{-1}. Although the value of γ depends on both the temperature and the generation rate, it is important to note that, at an intermediate generation rate of $G=10^{19}$ cm^{-3}s^{-1}, γ is about 0.5 in the temperature region around 100 K, in good agreement with the experimental results.[4] At lower and higher tem-

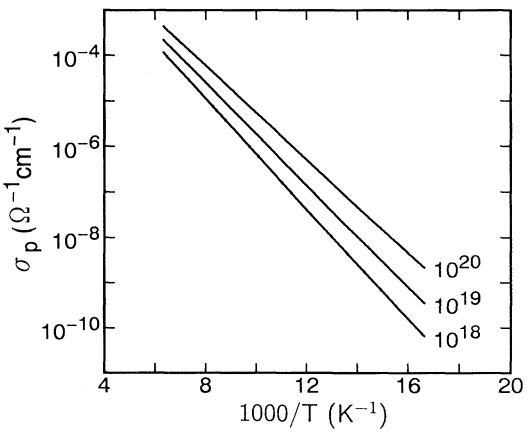

FIG. 2. Temperature dependence of the low-temperature photoconductivity calculated with the TTTR model for three carrier generation rates: 10^{18}, 10^{19}, and 10^{20} cm^{-3}s^{-1}.

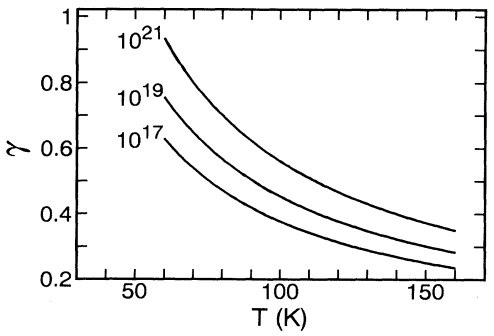

FIG. 3. Temperature dependence of the exponent γ defined by Eq. (17) at three carrier generation rates: 10^{17}, 10^{19}, and 10^{21} $cm^{-3}s^{-1}$.

peratures, other recombination and transport mechanisms may need to be taken into account and, thus, the value of γ can be quite different from that indicated in Fig. 3.

We have seen that the features exhibited by the photoconductivity of a-Si:H in the temperature region around 100 K can be predicted by the TTTR model. It should be pointed out, however, that although the results are qualitatively independent of the values chosen for the parameters involved in the model, the details of the results, such as the calculated magnitudes of the quantities, depend critically on the values of the parameters. As mentioned in Sec. II, a large influence on the activation energy, and thus on the photoconductivity, comes from T_c and R_0. Figure 4 compares the photoconductivities calculated for $G=10^{19}$ $cm^{-3}s^{-1}$ with $T_c=300$ K and with $T_c=500$ K. One can see that the photoconductivity is decreased by many orders of magnitude when T_c is changed from 300 to 500 K. It can be shown that γ also increases with increasing T_c.

The strong effect of R_0 on the photoconductivity can be seen from the results of Fig. 5, where the photoconductivities for $R_0=8.5$ and 15 Å are plotted as a function of temperature. It is clear from Eq. (12) that B and R_0

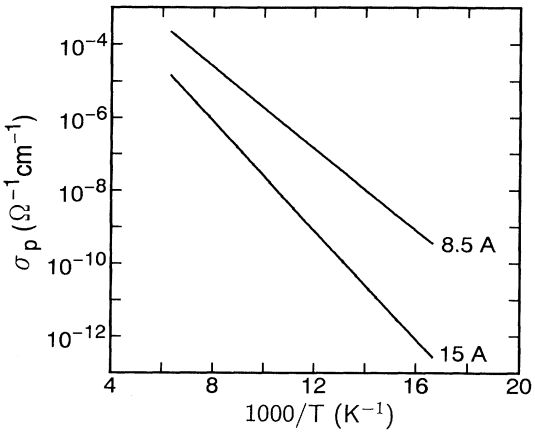

FIG. 5. Effect of the value of the localization length on the photoconductivity. The localization lengths used in the calculations are indicated in the figure.

play an opposite role in determining the photoconductivity; the effect of increasing B on the photoconductivity is equivalent to that of decreasing R_0. Thus, the choice of the value for B is not trivial; a small variation in B will result in quite a significant change in the photoconductivity.

IV. DIFFICULTY WITH THE TTTR MODEL

Despite the success of the tail-to-tail-tunneling-recombination (TTTR) model in accounting for many of the features exhibited by the photoconductivity of a-Si:H in the temperature region of interest here, the model is not entirely free of difficulty. One aspect that we have not addressed so far is the absolute magnitude of the photoconductivity. It is important to compare the theoretical results with the experimental results in a quantitative manner. Such a comparison is made in Fig. 6, where we show the photoconductivity calculated for a carrier generation rate of $G=10^{19}$ $cm^{-3}s^{-1}$ using the same set of

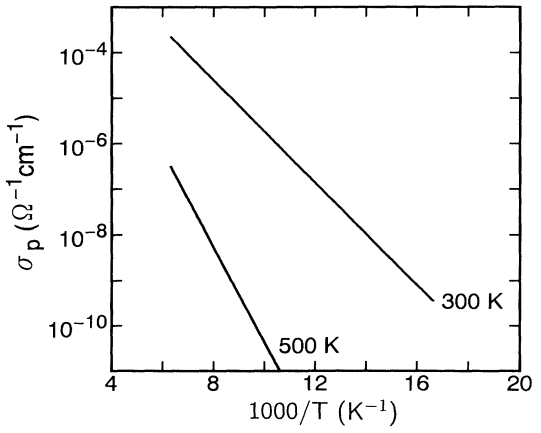

FIG. 4. Effect of the value of the characteristic temperature T_c of the band tail on the photoconductivity. The characteristic temperatures used in the calculations are indicated in the figure.

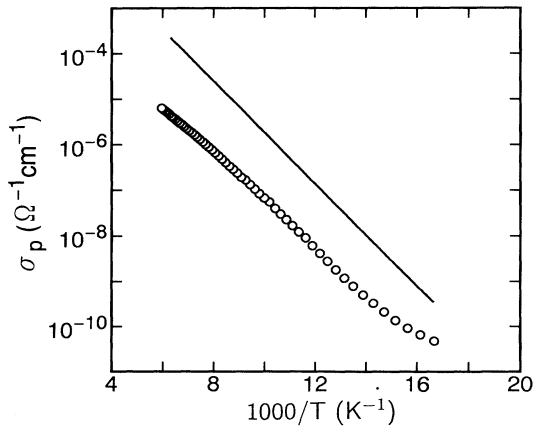

FIG. 6. Comparison of the photoconductivity predicted by the TTTR model with the experimental data. Solid line: theoretical calculation; data: experimental result.

parameter values given at the end of Sec. III A (solid line), together with the photoconductivity measured at the same generation rate.[1] It seems that the TTTR model is deficient, because the photoconductivity predicted by the model is significantly larger than that measured.

However, the difficulty may not be as serious as it seems. The value assumed for the electron mobility in the calculation may be higher than its actual value. There has been no technique with which the carrier mobilities of *a*-Si can be measured directly. The value commonly adopted for the mobility is deduced from model fitting of the drift-mobility data,[16,22] where the free-carrier mobility is actually treated as an adjustable parameter. Had the mobility been taken to be $\mu_e = 1$ $cm^2 V^{-1} s^{-1}$, the photoconductivity would have been ten times lower, which is in much better agreement with the experimental result.

Nevertheless, the discrepancy between theory and experiment is not entirely resolved because it is not clear whether $\mu_e = 1$ $cm^2 V^{-1} s^{-1}$ is still a reasonable assumption. Further study is therefore needed.

V. DISCUSSION

It is important to note that a basic assumption made in our discussion is that the occupancy of the band-tail states can be described in terms of a special energy level—the filling level, similar to the quasi-Fermi-level description.[15] In order for this description to be valid, it is essential that the tunneling recombination be nongeminate or substantially nongeminate. It is known that, for pulsed excitation, the tunneling recombination is geminate if the photocarrier density is low and nongeminate if the photocarrier density is high, the critical density being about 10^{18} cm^{-3}.[29,30] However, in a steady-state-photoconductivity experiment, the excitation is carried out with continuous-wave (CW) illumination. Dunstan has shown that, for CW excitation, the tunneling recombination occurs between distant pairs, i.e., is nongeminate.[31] Considerable experimental evidence is available for the dominance of nongeminate tunneling recombination under CW excitation at low temperatures.[10,32,33]

Another assumption which is essential to the TTTR model is that the ratio of the numbers of radiative- and nonradiative-recombination channels does not change with temperature, which is equivalent to the assumption that the photoluminescence quantum efficiency η_{PL} is temperature independent. Experiments show that, normally, η_{PL} depends on temperature even at low temperatures.[19] However, we note that the dependence of η_{PL} on temperature is rather weak below about 140 K,[28,34] indicating that the assumption that η_{PL} is temperature independent is probably valid for the temperatures of interest in this paper.

The TTTR model is also consistent with other experimental results. It has been observed that, compared with the photoconductivity of *a*-Si:H prepared by the glow-discharge (GD) technique, the low-temperature photoconductivity is lower and its activation energy is larger in sputtered and in *p*-type *a*-Si:H.[28] These results can be readily understood in terms of the TTTR model. The conduction-band tail of sputtered *a*-Si:H is presumably broader than that of GD *a*-Si:H, which, according to the TTTR model, will give rise to a lower photoconductivity and a larger activation energy (see Fig. 4). The same argument applies to *p*-type *a*-Si:H. In *p*-type *a*-Si:H, the photoconductivity is due to holes and the band tail in question is the valence-band tail. It is well known that the valence-band tail is broader than the conduction-band tail.[16,35] As a result, the low-temperature photoconductivity will be lower and the photoconductivity activation energy larger in *p*-type *a*-Si:H.

It is tempting to suggest that the TTTR model might also apply to other amorphous semiconductors, since the low-temperature photoconductivities of different materials show the same general features.[9,36] We note, however, that the photoconductivity of chalcogenide glasses does not show thermal quenching.[37] Since thermal quenching of photoconductivity in *a*-Si:H has been shown to result from a transition from band-tail-states-dominated to detect-dominated recombination,[1] it is not clear whether there exists any temperature region in chalcogenide glasses where the recombination is dominated by the band-tail states. Therefore, great caution should be taken in applying the TTTR model to materials other than *a*-Si:H.

VI. SUMMARY

A model has been proposed to interpret the photoconductivity of *a*-Si:H in the low-temperature region between ~ 50 and ~ 150 K, where the photoconductivity is found to increase rapidly with temperature and usually exhibits a thermally activated behavior. In this model, the recombination takes place by direct tunneling between electrons trapped in the conduction-band tail and holes trapped in the valence-band tail, whereas the photoconductivity is due to electron conduction in extended states. It is shown that this tail-to-tail-tunneling-recombination model can account for many of the features exhibited by the photoconductivity of *a*-Si:H in the low-temperature region. However, a quantitative comparison has revealed that the magnitude of the photoconductivity predicted by the model tends to be larger than that measured. It is suggested that the uncertainty in the value taken for the electron mobility may be responsible, at least partly, for this discrepancy.

ACKNOWLEDGMENT

The authors benefited from discussions with Professor H. Fritzsche of the University of Chicago.

*Present address: Department of Electrical and Computer Engineering, Faculty of Technology, Kanazawa University, 2-40-20 Kodatsuno, Kanazawa 920, Japan.

[1] J.-H. Zhou and S. R. Elliott, Philos. Mag. B **66**, 801 (1992).

[2] H. Dersch, L. Schweitzer, and J. Stuke, Phys. Rev. B **28**, 4678 (1983).

[3] P. E. Vanier, A. E. Delahoy, and R. W. Griffith, J. Appl. Phys. **52**, 5235 (1981).

[4]A. Vomvas and H. Fritzsche, J. Non-Cryst. Solids **97&98**, 823 (1987).
[5]H. Fritzsche, M. Q. Tran, B.-G. Yoon, and D.-Z. Chi, J. Non-Cryst. Solids **137&138**, 467 (1991).
[6]R. Carius, W. Fuhs, and K. Weber, in *Disordered Semiconductors,* edited by M. A. Kastner, G. A. Thomas, and S. R. Ovshinsky (Plenum, New York, 1987), p. 369.
[7]W. E. Spear and C. S. Cloude, Philos. Mag. Lett. **55**, 271 (1987).
[8]B. I. Shklovskii, H. Fritzsche, and S. B. Baranovskii, Phys. Rev. Lett. **62**, 2989 (1989).
[9]H. Fritzsche, J. Non-Cryst. Solids **114**, 1 (1989).
[10]T. M. Searle, Philos. Mag. Lett. **61**, 251 (1990).
[11]M. Stutzmann, W. B. Jackson, and C. C. Tsai, Phys. Rev. B **32**, 23 (1985), and references therein.
[12]T. J. McMahon and J. P. Xi, Phys. Rev. B **34**, 2475 (1986).
[13]F. Vaillant, D. Jousse, and J-C. Bruyere, Philos. Mag. B **57**, 649 (1988).
[14]T. Smail and T. Mohammed-Brahim, Philos. Mag. B **64**, 675 (1991).
[15]A. Rose, *Concepts in Photoconductivity and Allied Problems* (Wiley, New York, 1963).
[16]T. Tiedje, in *Semiconductors and Semimetals,* edited by J. I. Pankove (Academic, Orlando, 1984), Vol. 21, Pt. C, p. 207.
[17]C. Main, R. Russell, J. Berkin, and J. M. Marshall, Philos. Mag. Lett. **55**, 189 (1987).
[18]W. Fuhs, J. Non-Cryst. Solids **77&78**, 593 (1985).
[19]R. A. Street, in *Semiconductors and Semimetals* (Ref. 16), Vol. 21, Pt. B, p. 197.
[20]R. A. Street, J. C. Knight, and D. K. Biegelsen, Phys. Rev. B **18**, 1880 (1978).
[21]H. Reiss, J. Chem. Phys. **25**, 400 (1956).
[22]W. E. Spear, J. Non-Cryst. Solids **59&60**, 1 (1983).
[23]M. Silver, L. Cohen, and D. Adler, Phys. Rev. B **24**, 4855 (1981).
[24]T. S. Nashashibi, I. G. Austin, and T. M. Searle, Philos. Mag. **35**, 831 (1977).
[25]R. W. Collins and W. Paul, Phys. Rev. B **25**, 5257 (1982).
[26]B. A. Wilson and T. P. Kerwin, Phys. Rev. B **25**, 5276 (1982).
[27]W. B. Jackson and R. J. Nemanich, J. Non-Cryst. Solids **59&60**, 353 (1983).
[28]M. Hoheisel, R. Carius, and W. Fuhs, J. Non-Cryst. Solids **59&60**, 457 (1983).
[29]C. Tsang and R. A. Street, Phys. Rev. B **19**, 3027 (1979).
[30]R. A. Street and D. K. Biegelsen, Solid State Commun. **44**, 501 (1982).
[31]D. J. Dunstan, Philos. Mag. B **46**, 579 (1982).
[32]F. Boulitrop and D. J. Dunstan, Solid State Commun. **44**, 841 (1982).
[33]M. Bort, R. Carius, and W. Fuhs, J. Non-Cryst. Solids **114**, 280 (1989).
[34]R. W. Collins, M. A. Paesler, and W. Paul, Solid State Commun. **34**, 833 (1980).
[35]R. A. Street, *Hydrogenated Amorphous Silicon* (Cambridge University Press, Cambridge, 1991).
[36]R. E. Johanson, H. Fritzsche, and A. Vomvas, J. Non-Cryst. Solids **114**, 274 (1989).
[37]N. F. Mott and E. A. Davis, *Electronic Processes in Non-Crystalline Materials,* 2nd ed. (Oxford University Press, Oxford, 1979).